Article

J. Biol. Regul. Homeost. Agents. 2024; 38(6): 4653–4662
https://doi.org/10.23812/j.biol.regul.homeost.agents.20243806.370

Improvement of M1 Polarization and Gut Flora with MiR-124 Agonist in HAP Mice

Xiaoying Zhang[1], Xingyu Rao[2], Guodong Yang[2,*], Yulin Chen[2], Zhao Mu[2], Haiyue Zhou[2], Luoyao Zhang[2]

[1]School of Basic Medicine and Forensic Sciences, North Sichuan Medical College, 637000 Nanchong, Sichuan, China
[2]Department of Gastroenterology and Hepatology, Affiliated Hospital of North Sichuan Medical College, 637000 Nanchong, Sichuan, China
*Correspondence: ygd_ld2006@163.com (Guodong Yang)
Submitted: 17 March 2023 Revised: 24 April 2023 Accepted: 6 June 2023 Published: 1 June 2024

Background: Hyperlipidemic acute pancreatitis (HAP) is characterized by high triglyceride (TG) and acute pancreatitis (AP), and is closely related to intestinal microflora. MiR-124 was found to have a significant regulatory relationship with chronic pancreatitis. Here, the study aimed to investigate the protection effect of miR-124 agonist in HAP.
Methods: HAP was induced in mice using a high-fat diet (HFD) and cerulein. We evaluated the biochemical and morphological protective effects of miR-124 in HAP mice. miR-124 expression in the serum and pancreas was quantified by real-time quantitative PCR (qRT-PCR). Cluster of differentiation 68 (CD68) expression in pancreatic macrophages was detected by immunohistochemistry. Colonic flora was analyzed using High-Throughput Sequencing. Flow cytometry was performed to determine macrophage polarization. Serum inflammatory cytokines were measured using enzyme-linked immunosorbent assay (ELISA). Western blot (WB) was performed to detect protein expression.
Results: The results revealed that miR-124 expression was downregulated in HAP mice ($p < 0.001$), which exhibited pathological injury and inflammatory cell infiltration in the pancreas. However, this status was inhibited by miR-124 agonist treatment. High-throughput sequencing of 16S rDNA demonstrated that miR-124 agonist treatment significantly reversed HAP-induced gut dysbiosis. Using Linear discriminant analysis Effect Size (LEfSe) analysis, we found that *Rikenellaceae* was the key species in the miR-124 agonist treatment of HAP. Finally, we found that the treatment with the miR-124 agonist promoted macrophage polarization toward M2 ($p < 0.05$) and inhibited the inflammatory response ($p < 0.05$) in HAP mice.
Conclusion: MiR-124 agonists improve HAP by attenuating inflammatory reactions, regulating macrophage polarization, and rebalancing the intestinal microbiota.

Keywords: hyperlipidemia acute pancreatitis; high-fat diet; miR-124; intestinal microbiota

Introduction

A pancreas inflammatory process, acute pancreatitis (AP), can lead to severe acute pancreatitis (SAP) and systemic inflammatory response syndrome (SIRS), putting life at risk [1,2]. One study reported SAP mortality rates of up to 25%, and 75–80% of self-limiting mild forms can progress into serious forms [3,4]. Macrophage activation is closely associated with AP severity [5], as pro-inflammatory cytokines like tumor necrosis factor-α (TNF-α) and play a role in its development [6–8]. Furthermore, when the pancreas is damaged, macrophages, and neutrophils migrating migrate to the pancreatic interstitial space, which further increase the production of various inflammatory mediators [9,10]. Hyperlipidemic acute pancreatitis (HAP) is characterized by high triglyceride (TG) and AP [11] and is more severe than AP [12].

The pancreas and intestines are the major initial sites of AP [13], and recent studies suggest that the intestinal microbiota is involved in the occurrence and development of pancreatitis, with an imbalance in the intestinal microbiota promoting AP development [14–16]. Hyperlipidemia is often accompanied by an imbalance in the intestinal microflora, which exacerbates lipid metabolism disorders and creates a vicious cycle [17,18]. Therefore, the intestinal microflora is closely related to the occurrence of HAP.

Several studies have indicated the crucial role of miRNAs, including miR-7, miR-9, miR-122, miR-92b, miR-10a, and miR-141, in the development of AP [19,20]. Modulating miRNAs in vivo offers a new approach to AP intervention [21–23]. Among them, miR-124 has been shown to play a significant role in various diseases in animal experiments [24–26]. Specifically, miR-124 has been linked to pancreatic development, inflammation, and cancer [27,28]. The miR-124 downregulation is strongly linked to poor prognosis in patients with pancreatic ductal adenocarcinoma [29]. Moreover, miR-124 has a significant regulatory relationship with chronic pancreatitis, indicating its poten-

Journal of
BIOLOGICAL REGULATORS
and Homeostatic Agents

tial as a diagnostic and therapeutic target for chronic pancreatitis [30]. Therefore, miR-124 could serve as an important regulator of pancreatic diseases and play a vital role in their treatment. However, the role of miR-124 in HAP remains unclear.

In this study, we established a mouse model of HAP by administering a high-fat diet (HFD) and cerulein to investigate the effect of miR-124 on HAP in mice. We also explored the protective effects of miR-124 from the perspective of intestinal microflora and macrophage polarization.

Method

Animal and Experimental Model

A total of 48 male C57BL/6J mice at 6 weeks of age (18 ± 2 g) were obtained from Chengdu Dashuo Experimental Animal Co., Ltd. (certificate No. SCXK201302, Sichuan, China) and housed under specific pathogen-free (SPF) conditions. All animal experimental procedures were performed and approved by the Ethics and Animal Welfare Committee of the West China Hospital of Sichuan University (Chengdu, Sichuan, China) (no.20220412010).

First Animal Experiment

In this experiment, eighteen male C57BL/6J mice were randomly divided into groups (n = 6) of Chow, HFD, and HFD+cerulein. The Chow group was fed a normal chow diet containing 10% kcal from fat, while the other two groups were given an HFD containing 54% kcal from fat. After 8 weeks of feeding, twice intraperitoneal injections on the mice were performed with saline or cerulein (40 μg/kg, diluted in saline) (C9026, Sigma, St Louis, MO, USA) at 2-hour intervals. Amylase test indicated the all HFD model has been successfully constructed. 1 hour after the last cerulein injection, the mice were deeply anesthetized by 1% pentobarbital sodium (Y0002194, Sigma, St Louis, MO, USA), and plasma and pancreatic tissue samples were prepared for later analysis instantly. Finally, the mice were euthanized by dislocation of neck.

Second Animal Experiment

In this experiment, thirty male C57BL/6J mice were randomly divided into groups (n = 6) of Chow, Chow+miR-124 agonist, HFD+cerulein, and HFD+miR-124 agonist+cerulein. The Chow and Chow+miR-124 agonist groups were fed a normal chow diet (fat: 10% kcal), while the other three groups were given an HFD diet (fat: 54% kcal). After 8 weeks of feeding, the mice received caudal vein injections of saline or miR-124 agonist (80 mg/kg, diluted in ddH_2O) (miR40004527-4-5, RiboBio, Guangzhou, China) once a week for 3 weeks. One day after the final miR-124 agonist injection, twice intraperitoneal injections on the mice were performed with saline or 40 μg/kg cerulein at 2-hour intervals. 12 hours after the final cerulein injection, 1% pentobarbital sodium was used to anesthetize the mice deeply. Finally, the plasma, colon contents, and tissue samples were then prepared for later analysis, and the mice were euthanized by dislocation of neck.

The colon contents, a portion of colon tissue, pancreas tissue and serum were rapidly snap-frozen and stored at –80 °C. The remaining colon and pancreatic tissues were quickly removed and fixed in 10% formalin (R03379, Sigma, St Louis, MO, USA) for later analysis using Haematoxylin-Eosin (H&E) staining and immunohistochemistry (IHC).

Measurement of TC, TG, and Amylase in Serum

An automatic biochemistry analyzer (7180, Hitachi, Tokyo, Japan) was used to detect triglyceride (TG), total cholesterol (TC), and serum amylase activity.

H&E Staining

Colon and pancreatic tissues were processed in a series of standard procedures to prepared 4-mm slices, including fixation, embedding and section. The paraffin sections were dewaxed in xylene, rehydrated, and stained with hematoxylin and eosin (Beyotime, Wuhan, China). A bright-field Nikon Eclipse-600 microscope (Nikon, Tokyo, Japan) was used to observe the sections and photographed.

Real Time Quantitative PCR (qPCR)

Total RNA of serum or pancreas in each group was isolated by TRIZOL (NP0007, Invitrogen, Carlsbad, CA, USA), and cDNA synthesis was performed using a reverse transcription kit (6210A, Takara, Beijing, China). qPCR was performed to quantify the miR-124 expression levels. The relative mRNA expression levels were normalized to β-actin, using the following primers: *miR-124* forward: 5′-GTCGTATCCAGTGCGTGTCGTGGAGTCGGCAATTGCACTGGATACGACGGCATTCA-3′; β-actin forward: 5′-GAAGATCAAGATCATTGCTCC-3′ and β-actin reverse: 5′-TACTCCTGCTTGCTGATCCA-3′. The results of qPCR were expressed as $2^{-\Delta\Delta Ct}$.

IHC Detection

IHC was applied to measure the cluster of differentiation 68 (CD68) expression levels in pancreatic macrophages. The sections were first blocked in phosphate-buffered saline (PBS) (P3813, Sigma, St Louis, MO, USA) for 30 minutes at temperature of 20–25 °C, followed by an incubation of primary antibody CD68 (1:100, Ab283654, Abcam, Cambridge, UK) at 4 °C. On the second day, using the secondary antibody (1:200, ZB-2306, Zhongshan Jinqiao, Beijing, China) to amplify signal. Finally, Image PeroPlus 6.0 (IPP 6.0, Media Cybernetics, Inc., Rockville, MD, USA) was used to quantify the CD68 expression level at a magnification of ×200. DAB area/tissue area analyzed*100% was used to quantify IHC.

DNA Extraction and Intestinal Microbiota Sequencing

The colon contents of the mice were sent to a commercial laboratory (Shanghai Paisenuo Medical Laboratory Co. Ltd., Shanghai, China) for intestinal microbiota sequencing. The following steps were performed: DNA was extracted from the colon contents and its purity was examined using 1.2% agarose gel (A9539, Sigma, St Louis, MO, USA) electrophoresis. PCR was used to amplify the target fragments, specifically the V3 and V4 regions of the bacterial 16S rRNA gene. The purified PCR products were measured by using the Quant-iT PicoGreen dsDNA Assay Kit (P7589, Life Technologies, Carlsbad, CA, USA) and sequenced on an Illumina MiSeq platform (San Diego, CA, USA). The alpha index was analyzed using QIIME2 software and the intestinal microbiota composition was analyzed using QIIME2 software and the R ggplot2 package. The Linear discriminant analysis Effect Size (LEfSe) analysis was performed using the Python LEfSe package (Huttenhower Lab, Cambridge, MA, USA).

Flow Cytometry

Flow cytometry was performed using a standard protocol. The pancreas was minced in RPMI-1640 (R4130, Sigma, St Louis, MO, USA) supplemented with appropriate additives and centrifuged to generate cells. Pancreatic macrophages were subjected to flow cytometry using fluorochrome-conjugated antibodies against CD86 (Ab239075, Abcam, Cambridge, UK), CD206 (Ab270647, Abcam, Cambridge, UK), and F4/80 (111602, BioLegend, San Diego, CA, USA). Flow cytometry (Cytoflex, Brea, CA, USA) and Kaluza software (Beckman Coulter, Brea, CA, USA) were used to analyze all stained cells and report the resulting data.

Enzyme-Linked Immunosorbent Assay (ELISA)

The levels of lipopolysaccharide (LPS), monocyte chemoattractant protein (MCP-1), TNF-α, interleukin (IL)-6, IL-4, IL-10, and IL-13 cytokines in the serum were measured using enzyme-linked immunosorbent assay (ELISA) kits (DY870-05, MJE00B, MTA00B, M6000B, M4000B, DY417, 213-ILB, RD, MN, USA). A microplate reader (WD-2102B, Beijing Liuyi Biotechnology, Beijing, China) was employed to measure the absorbance at 450 nm.

Western Blot

After the extracting of total pancreatic protein, the Pierce BCA Protein Assay Kit (23235, Thermo, Waltham, MA, USA) was used to measure the protein concentration of samples following the manufacturer's instructions. Next, protein was separated using sodium dodecyl sulfate-polyacrylamide gel electrophoresis and transferred to PVDF membranes. The membranes were then blocked with 5% BSA (w/v) and incubated with primary antibodies against p-p65 (1:1000, AF2006, Affinity, Miami, FL, USA), p65 (1:1000, ab32536, Abcam, Cambridge, UK), Signal transduction and activator of transcription (STAT)6 (1:1000, ab32108, Abcam, Cambridge, UK), p-STAT6 (1:1000, AF3301, Affinity, Miami, FL, USA), and beta-actin (1:5000, ab8226, Abcam, Cambridge, UK) overnight at 4 °C. After washing thrice with TBST, the bands were incubated with secondary antibodies against goat Anti-Mouse IgG H&L (1:10000, ab175783 Abcam, Cambridge, UK) or goat Anti-Rabbit IgG H&L (1:20000, ab97051, Abcam, Cambridge, UK). The reaction was visualized using an ECL kit (64-201BP, Millipore, Boston, MA, USA) and an imaging system (Tanon 5200, Shanghai, China). All relative proteins expression levels were normalized to β-actin.

Statistical Analysis

The statistical analysis was performed using SPSS 19 software (IBM, New York, NY, USA). The data are presented as mean $\pm$ standard deviation (SD). The data comparisons among the groups were analyzed using one-way ANOVA, followed by the LSD test. Each experiment was repeated at least three times. A p-value < 0.05 was considered statistically significant.

Results

Expression of MiR-124 in HFD-Induced AP

The results of the first animal experiment are presented in Fig. 1. As illustrated in Fig. 1A, miR-124 levels in the serum ($p < 0.001$) and pancreas ($p < 0.01$) were obviously reduced following HFD treatment. Additionally, the HFD+cerulein group had lower miR-124 in the serum ($p < 0.01$) and pancreas ($p < 0.05$) compared to the HFD group. The TG ($p < 0.05$) and TC ($p < 0.01$) levels of serum were obviously higher in both HFD-fed groups (with or without cerulein) than those in the control group (Fig. 1B), and no significant differences in serum TC and TG levels were observed between the HFD and HFD+cerulein groups. Histological examination by H&E staining showed the infiltration of inflammatory cells and degeneration and necrosis of islets and acinar epithelial cells in the HFD group, and an increase in these histological features was observed in the HFD+cerulein group, as depicted in Fig. 1C. Fig. 1D shows that there was no difference in amylase activity between the control and HFD groups; however, HFD-fed mice treated with cerulein showed a significant increase in amylase activity compared to the control group ($p < 0.05$). Furthermore, Fig. 1E indicates that HFD-fed mice treated with cerulein significantly increase the CD68 expression level in the pancreas compared to control mice ($p < 0.05$), whereas HFD-fed mice did not exhibit a noticeable increase of the CD68-positive cell number.

Journal of
BIOLOGICAL REGULATORS
and Homeostatic Agents

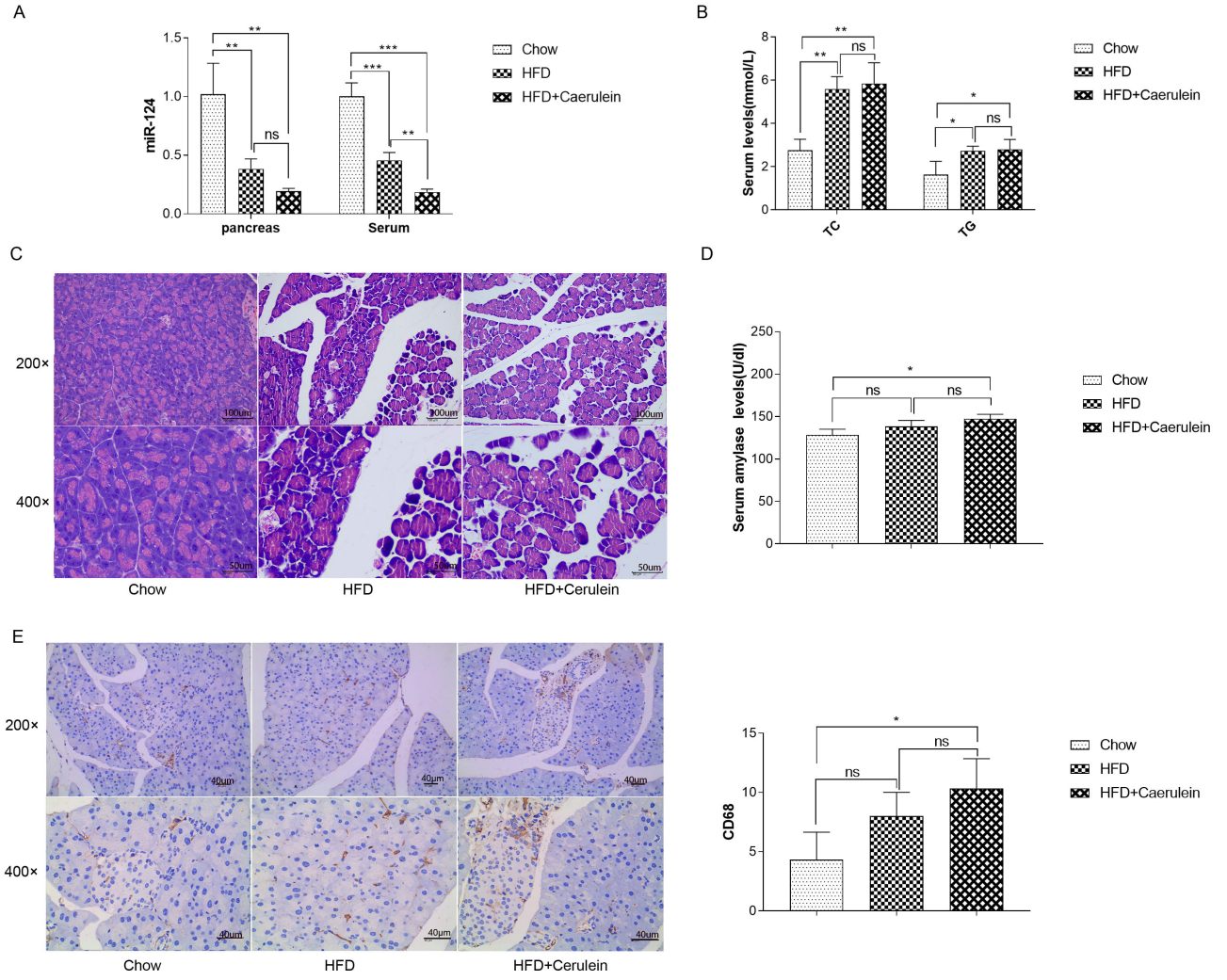

Fig. 1. The miR-124 expression in serum and pancreas, and the result of serum biochemical, Haematoxylin-Eosin (H&E) staining and immunohistochemistry (IHC). (A) MiR-124 expression in serum and pancreas. (B) Cholesterol (TC), triglyceride (TG) levels in serum. (C) H&E of the pancreas. (D) Serum amylase levels. (E) IHC staining and quantification of CD68 for macrophages infiltrating the pancreas. Samples (n = 3) and we indicated the * $p < 0.05$, ** $p < 0.01$, *** $p < 0.001$, ns $p > 0.05$. HFD, high-fat diet; CD68, cluster of differentiation 68.

Protection Effect of MiR-124 Agonist Treatment on HAP

The second animal experiment aimed to investigate the protective effects of miR-124 agonist treatment on HAP. The HAP mouse model was induced by HFD feeding and cerulein stimulation, as shown in Fig. 2. The results revealed that miR-124 agonist treatment led to significant increases in miR-124 levels in the pancreas and serum of normal ($p < 0.001$) and HAP mice ($p < 0.05$) (Fig. 2A). However, there were no significant differences in serum TC and TG levels following miR-124 agonist treatment in either normal or HAP mice (Fig. 2B). Histological analysis showed that miR-124 agonist treatment significantly decreased islet cell degeneration, necrosis, and inflammatory cell infiltration in HAP mice, whereas pancreatic samples from the chow+miR-124 agonist group showed degeneration and necrosis of only a few acinar epithelial cells and infiltration of a few inflammatory cells (Fig. 2C). The analysis of serum amylase activity revealed that miR-124 agonist treatment resulted in a decrease in HAP mice ($p < 0.01$), although there was no statistical significance (Fig. 2D). Furthermore, miR-124 agonist treatment significantly decreased the number of CD68-positive macrophages in HAP mice ($p < 0.05$), while no significant difference was observed in normal mice (Fig. 2E). These data suggest that miR-124 agonist treatment may inhibit amylase activity and macrophage infiltration in the pancreas of HAP mice, but has no regulatory effect on TC and TG levels.

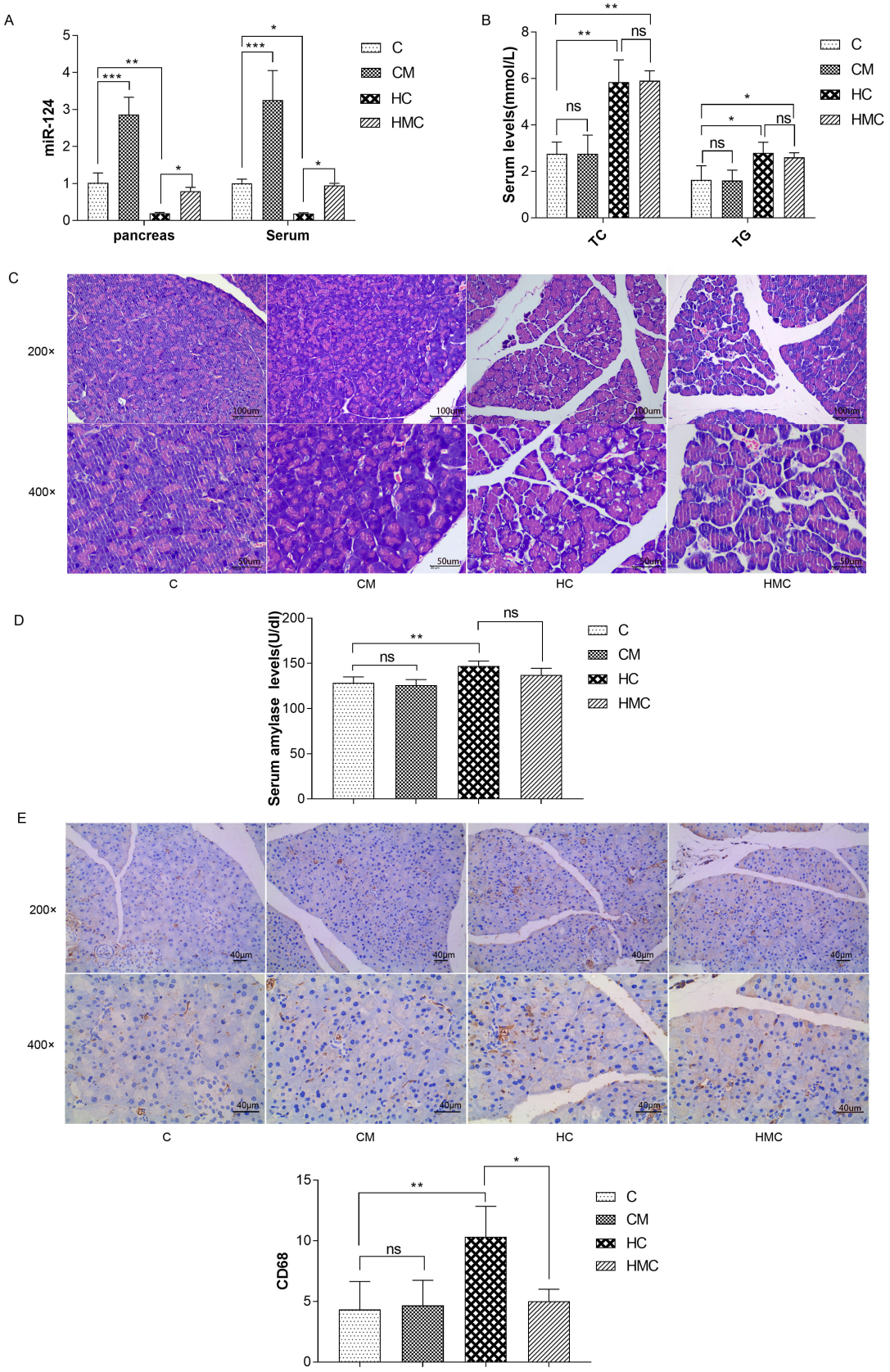

Fig. 2. MiR-124 agonist inhibited HAP. There were four groups: Chow (C), Chow+miR-124 agonist (CM), HFD+cerulean (HC), and HFD+miR-124 agonist+cerulean (HMC). (A) MiR-124 expression in serum and pancreas. (B) TC, TG levels in serum. (C) H&E staining for the pancreas. (D) Serum amylase levels. (E) IHC staining and quantification of CD68 for macrophages infiltrating the pancreas. Samples (n = 3) and we indicated the * $p < 0.05$, ** $p < 0.01$, *** $p < 0.001$, ns $p > 0.05$.

Journal of
BIOLOGICAL REGULATORS
and Homeostatic Agents

Effects of MiR-124 Agonist Treatment on Intestinal Microbiota and Mucosa in HAP Mice

Fig. 3A shows that treatment with the miR-124 agonist decreased Chao1 and Shannon indices in normal mice, whereas Fig. 3B shows that HAP mice had an increased relative abundance of *Firmicutes* and *Actinobacteria* and a decreased relative abundance of *Bacteroidetes* at the phylum level compared to normal mice, which was reversed by miR-124 agonist treatment during the test. At the genus level, as shown in Fig. 3C, the miR-124 agonist treatment inhibited the changes in *Lactobacillus* and *Allobaculum* in HAP mice. LEfSe analysis was further performed with 2 as the threshold for the logarithmic LDA score for discriminative features, and Fig. 3D shows that *Rikenellaceae* was the common core microbiota in normal and miR-124-treated HAP mice compared to HAP mice. The H&E staining results in Fig. 3E show that the colonic mucosa of HAP mice had several inflammatory cells in the connective tissue and a large number of non-stained goblet cells in the glandular epithelium, whereas miR-124 agonist treatment resulted in a decrease in the histological signs of colon mucosal damage in HAP mice. Thus, our study demonstrated that miR-124 agonist treatment could improve the intestinal microbiota and protect the intestinal mucosa in HAP, and *Rikenellaceae* could be a key species in the treatment of HAP.

Effects of MiR-124 Agonist Treatment on Macrophage Activation in HAP Mice

Since macrophage activation plays a key role in the host inflammatory response, we investigated the abundance of M1 and M2 macrophages in this study (Fig. 4A). We found that the M1 macrophage population (F4/80+ CD86+) was obviously up-regulated in HC group ($p < 0.01$), whereas the M2 (F4/80+ CD206+) population was notably decreased in HC group compared to that in normal mice ($p < 0.05$). However, compared with the HC group, treatment with the miR-124 agonist inhibited M1 macrophage activation ($p < 0.01$) and promoted M2 macrophage activation ($p < 0.05$). In addition, we measured the levels of IL-6, LPS, MCP-1, and TNF-α in HAP mice ($p < 0.05$, $p < 0.05$, $p < 0.05$, $p < 0.05$) and found that miR-124 agonist treatment reduced their levels while increasing the expression of IL-4, IL-10, and IL-13 ($p < 0.05$, $p < 0.05$, $p < 0.01$), as shown in Fig. 4B. We also detected macrophage polarization and found an increase in p65 protein expression ($p < 0.01$) and a decrease in STAT6 protein expression ($p < 0.01$) (the obtained values of p-p65/pSTAT6 were normalized to those of p65/STAT6) in HC group compared with the C group (Fig. 4C). However, miR-124 agonist treatment reduced the protein expression of p65 ($p < 0.05$) and increased that of STAT6 ($p < 0.05$) in HAP mice. These results indicated that the miR-124 agonist promoted macrophage polarization toward M2 in HAP mice.

Discussion

Over the past few years, our understanding of AP has increased [31]. However, the relationship between HAP and miRNAs has not been extensively investigated. Therefore, in this study, we examined the levels of miR-124 in mice with HAP and the protective effects of miR-124 on HAP. Our results demonstrated that miR-124 levels are associated with HAP, as the levels of miR-124 in the serum and pancreas were decreased in HAP mice. Furthermore, miR-124 agonist treatment significantly reduced pancreatic damage, macrophage infiltration, and serum amylase activity in HAP mice, accompanied by a significant increase in miR-124 expression, indicating that miR-124 upregulation can inhibit HAP. Interestingly, the miR-124 agonist had no significant effect on the TG and TC levels in HAP mice.

Numerous studies have shown that changes in the intestinal microbiota are closely linked to the development and treatment of hyperlipidemia [32,33]. In this study, we observed that changes in the abundance of *Firmicutes* and *Bacteroidetes* in HAP mice were inhibited by treatment with the miR-124 agonist and that the miR-124 agonist increased the abundance of *Lactobacillus* and decreased the abundance of *Allobaculum* in HAP mice. These findings suggest that the miR-124 agonist may contribute to the establishment of a relatively stable microflora structure. As it is well-known that *Lactobacillales* play a vital role in improving obesity under HFD [34], and thus the miR-124 agonist may improve HAP by increasing the abundance of *Lactobacillus*. However, our LEfse analysis identified *Rikenellaceae* as the key species in the miR-124 agonist treatment of HAP, but more research is needed to support this view.

Serum levels of LPS are associated with an imbalance in the intestinal microbiota and changes in intestinal barrier permeability [35]. LPS produced by the intestinal microbiota activates inflammatory NF-κB through TLR4 in both humans and mice [36]. In our study, we observed that miR-124 agonist treatment improved colonic mucosal damage and reduced serum LPS levels in HAP mice, indicating that the miR-124 agonist not only improved the intestinal microbiota but also enhanced the intestinal mucosal barrier.

Interestingly, macrophages play a critical role in controlling the direction of immune responses, with M1 promoting pro-inflammatory and M2 promoting anti-inflammatory responses [37]. The activation of macrophages is associated with the severity of AP that act as important inflammatory cells [38]. A previous study suggested that miR-124 is a regulator of M2 polarization in various monocytic cell subsets [39], and upregulation of miR-124 could ameliorate inflammation [24–26]. In our study, we found that treatment with an miR-124 agonist inhibited the NF-κB signaling pathway, promoted the STAT6 signaling pathway, inhibited M1 macrophage activation, and promoted M2 macrophage activation in HAP mice. These data suggest that treatment with the miR-124

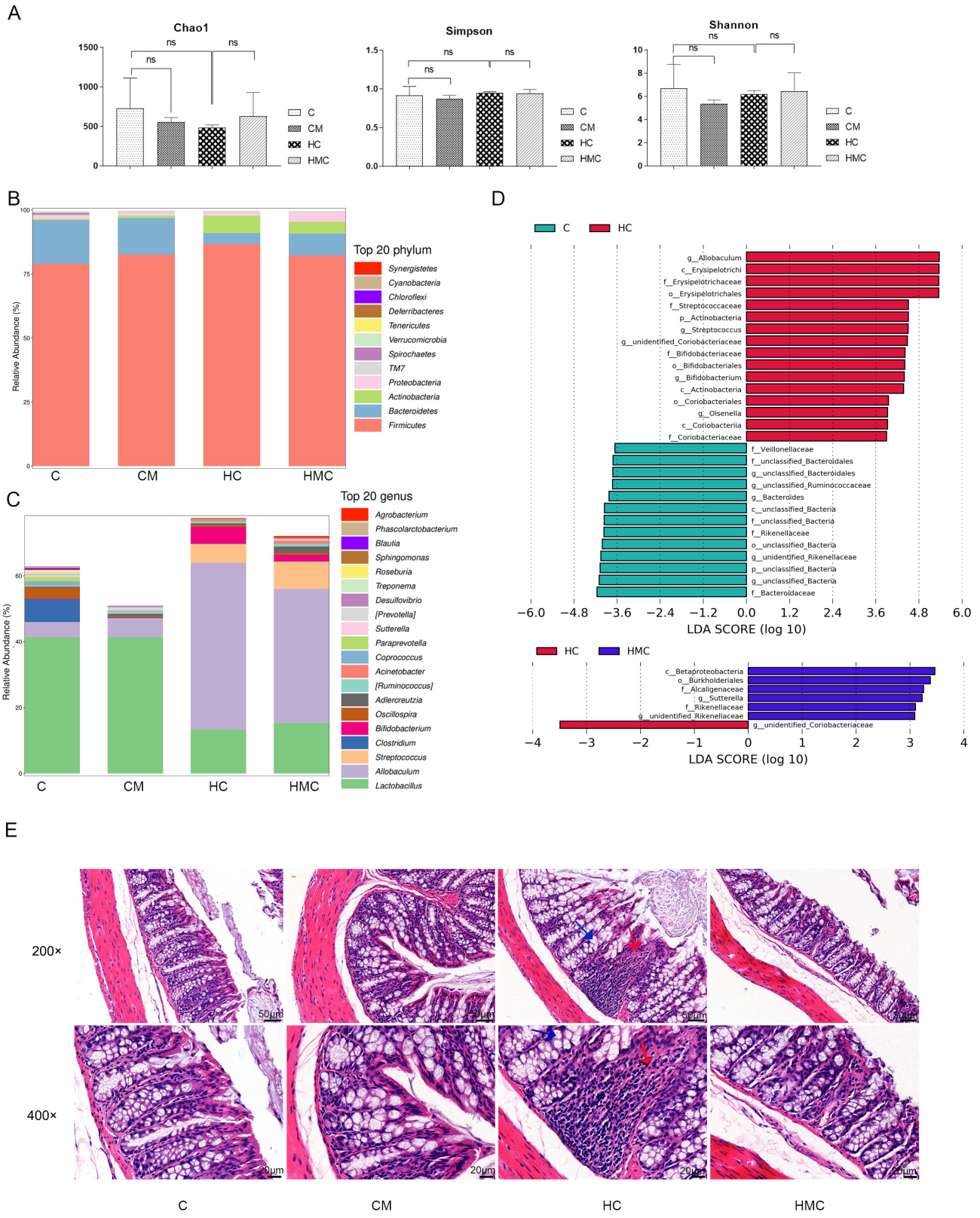

Fig. 3. MiR-124 agonist protected intestinal microbiota and intestinal mucosa in HAP. There were four groups: Chow (C), Chow+miR-124 agonist (CM), HFD+cerulean (HC), and HFD+miR-124 agonist+cerulean (HMC). (A) Alpha index. (B) Phylum level of community abundance. (C) Genus level of community abundance. (D) LEfse analysis. (E) H&E of the colon, 200× and 400×. The red arrows were inflammatory cells and the blue were goblet cells. Samples (n = 3) and we indicated ns $p > 0.05$. LEfSe, Linear discriminant analysis Effect Size.

Journal of
BIOLOGICAL REGULATORS
and Homeostatic Agents

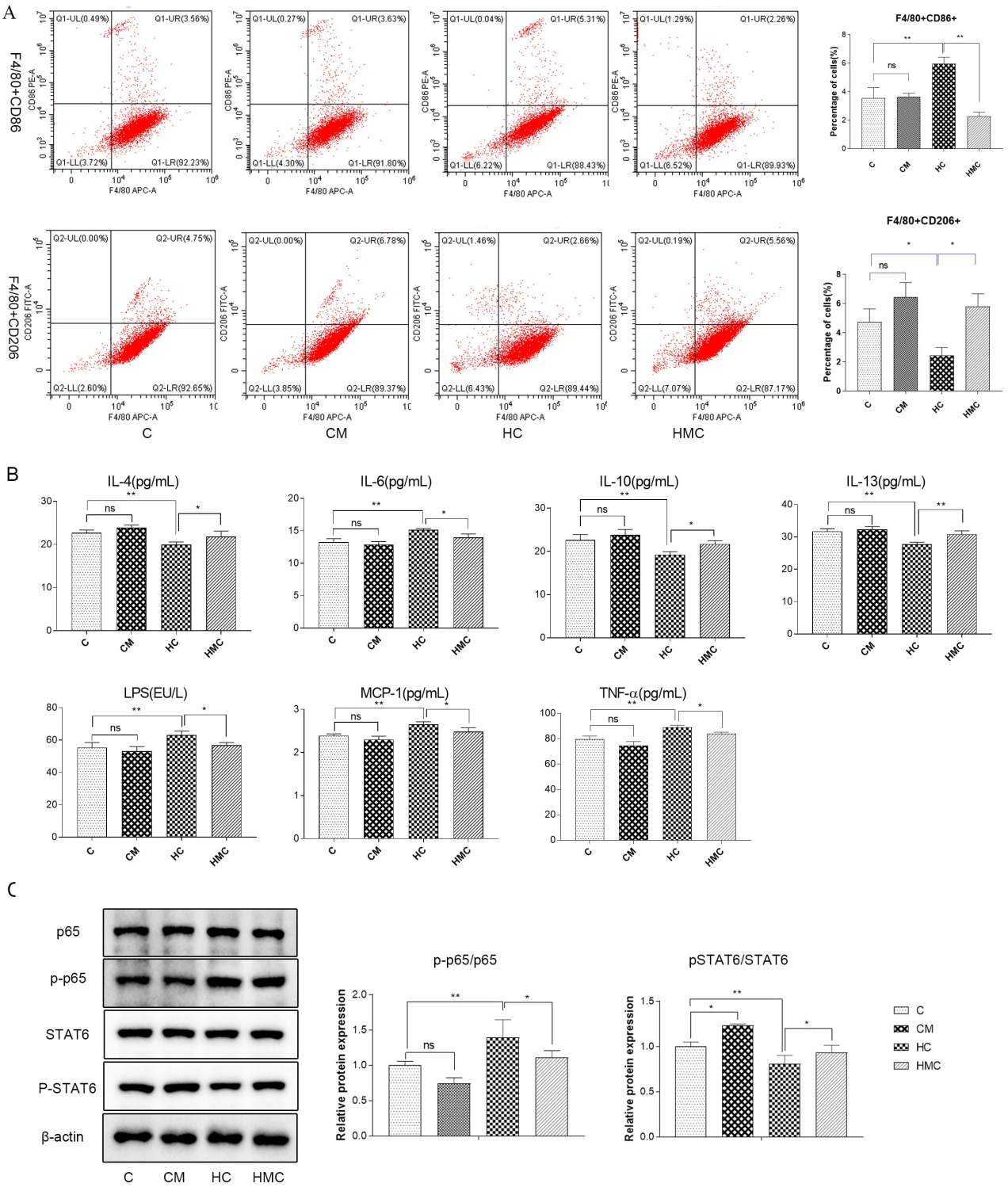

Fig. 4. MiR-124 agonist inhibited macrophagic activation and inflammatory cytokine expression in HFD-induced AP. There were four groups: Chow (C), Chow+miR-124 agonist (CM), HFD+cerulean (HC), and HFD+miR-124 agonist+cerulean (HMC). (A) Flow cytometric was performed to analyze the serum M1 (CD86) and M2 (CD206) macrophages activation levels. (B) Serum cytokines levels, including lipopolysaccharide (LPS), monocyte chemoattractant protein (MCP-1), tumor necrosis factor-α (TNF-α), interleukin (IL)-6, IL-4, IL-10, and IL-13. (C) WB analysis of p65, p-p65, signal transduction and activator of transcription (STAT)6, and p-STAT6 of the pancreas. The obtained values of p-p65/pSTAT6 were normalized to p65/STAT6. Samples (n = 3) and we indicated the * $p < 0.05$, ** $p < 0.01$, ns $p > 0.05$.

agonist can improve the inflammatory response in HAP by promoting macrophage polarization toward M2. Furthermore, macrophage activation induced by the miR-124 agonist in HAP may be associated with changes in serum LPS levels. A previous study has shown that LPS can bind to LPS-binding protein (LBP) and form the LPS/LBP complex, which activates M1 macrophage polarization through the TLR-4 signaling pathway [40].

Conclusion

In conclusion, this study confirms the anti-inflammatory properties of the miR-124 agonist in HAP, which may be related to M1/M2 polarization. Additionally, the miR-124 agonist also improves the intestinal microbiota in HAP mice, and the data obtained suggest that *Rikenellaceae* may be a key species. However, further studies are needed to determine whether miR-124 agonists, alone or in combination with other strategies, can be as effective in treating HAP in humans as they are in animal models of the disease.

Availability of Data and Materials

The data used to support the findings of this study are available from the corresponding author upon request.

Author Contributions

XZ, XR and GY contributed to the concept and designed the research study. XZ, GY, and YC performed the research. ZM contributed to the analysis and interpretation of the data. HZ and LZ provided help and advice on the WB experiments. All authors contributed to editorial changes in the manuscript. All authors read and approved the final manuscript. All authors have participated sufficiently in the work and agreed to be accountable for all aspects of the work.

Ethics Approval and Consent to Participate

All animal experimental procedures were performed and approved by the Ethics and Animal Welfare Committee of the West China Hospital of Sichuan University (Sichuan, China) (no.20220412010).

Acknowledgment

Not applicable.

Funding

This research was supported by the Doctoral Scientific Research Foundation of North Sichuan Medical College (CBY13-QD-05), Special Project of Science and Technology Strategic Cooperation between the City and the University (18SXHZ0371), the Research Development Program of North Sichuan Medical College (2022ZD005), and the 2023 Nanchong Science and Technology Special Program (23JCYJPT0056).

Conflict of Interest

The authors declare no conflict of interest.

References

[1] Sbeit W, Abu Elheja F, Msheiil B, Shahin A, Khoury S, Sbeit M, *et al*. Fatty pancreas was associated with a higher acute pancreatitis Systemic Inflammatory Response Syndrome score at hospital admission. European Journal of Gastroenterology & Hepatology. 2023; 35: 980–984.

[2] Li H, Wu D, Zhang H, Li P. New insights into regulatory cell death and acute pancreatitis. Heliyon. 2023; 9: e18036.

[3] Dervenis C, Johnson CD, Bassi C, Bradley E, Imrie CW, McMahon MJ, *et al*. Diagnosis, objective assessment of severity, and management of acute pancreatitis. Santorini consensus conference. International Journal of Pancreatology: Official Journal of the International Association of Pancreatology. 1999; 25: 195–210.

[4] Wu XN. Current concept of pathogenesis of severe acute pancreatitis. World Journal of Gastroenterology. 2000; 6: 32–36.

[5] Sheng LP, Han CQ, Ling X, Guo XW, Lin R, Ding Z. Proanthocyanidins suppress NLRP3 inflammasome and M1 macrophage polarization to alleviate severe acute pancreatitis in mice. Journal of Biochemical and Molecular Toxicology. 2023; 37: e23242.

[6] Duan F, Wang X, Wang H, Wang Y, Zhang Y, Chen J, *et al*. GDF11 ameliorates severe acute pancreatitis through modulating macrophage M1 and M2 polarization by targeting the TGFβR1/SMAD-2 pathway. International Immunopharmacology. 2022; 108: 108777.

[7] Shen D, Tang C, Zhu S, Huang G. Macrophage migration inhibitory factor is an early marker of severe acute pancreatitis based on the revised Atlanta classification. BMC Gastroenterology. 2021; 21: 34.

[8] Chen ZP, Huang HP, He XY, Wu BZ, Liu Y. Early continuous blood purification affects TNF-α, IL-1β, and IL-6 in patients with severe acute pancreatitis via inhibiting TLR4 signaling pathway. The Kaohsiung Journal of Medical Sciences. 2022; 38: 479–485.

[9] Zhang X, Yang G, Chen Y, Mu Z, Zhou H, Zhang L. Resveratrol pre-treatment alleviated caerulein-induced acute pancreatitis in high-fat diet-feeding mice via suppressing the NF-κB proinflammatory signaling and improving the gut microbiota. BMC Complementary Medicine and Therapies. 2022; 22: 189.

[10] Su YR, Hong YP, Mei FC, Wang CY, Li M, Zhou Y, *et al*. High-Fat Diet Aggravates the Intestinal Barrier Injury via TLR4-RIP3 Pathway in a Rat Model of Severe Acute Pancreatitis. Mediators of Inflammation. 2019; 2019: 2512687.

[11] Lin YF, Yao Y, Xu Y, Huang HB. Apheresis Technique for Acute Hyperlipidemic Pancreatitis: A Systemic Review and Meta-Analysis. Digestive Diseases and Sciences. 2023; 68: 948–956.

[12] Song X, Shi D, Cui Q, Yu S, Yang J, Song P, *et al*. Intensive insulin therapy versus plasmapheresis in the management of hypertriglyceridemia-induced acute pancreatitis (Bi-TPAI trial): study protocol for a randomized controlled trial. Trials. 2019; 20: 365.

[13] Wan YD, Zhu RX, Pan XT, Sun TW. Bile Acid Supplementation Improves Murine Pancreatitis in Association With the Gut Microbiota. Frontiers in Physiology. 2020; 11: 650.

Journal of
BIOLOGICAL REGULATORS
and Homeostatic Agents

[14] Tan C, Ling Z, Huang Y, Cao Y, Liu Q, Cai T, *et al*. Dysbiosis of Intestinal Microbiota Associated With Inflammation Involved in the Progression of Acute Pancreatitis. Pancreas. 2015; 44: 868–875.

[15] Wan YD, Zhu RX, Bian ZZ, Pan XT. Improvement of Gut Microbiota by Inhibition of P38 Mitogen-Activated Protein Kinase (MAPK) Signaling Pathway in Rats with Severe Acute Pancreatitis. Medical Science Monitor: International Medical Journal of Experimental and Clinical Research. 2019; 25: 4609–4616.

[16] Chen J, Huang C, Wang J, Zhou H, Lu Y, Lou L, *et al*. Dysbiosis of intestinal microbiota and decrease in paneth cell antimicrobial peptide level during acute necrotizing pancreatitis in rats. PloS One. 2017; 12: e0176583.

[17] Li Y, Lu X, Li X, Guo X, Sheng Y, Li Y, *et al*. Effects of *Agaricus blazei* Murrill polysaccharides on hyperlipidemic rats by regulation of intestinal microflora. Food Science & Nutrition. 2020; 8: 2758–2772.

[18] Shuang D, Wenfei Z, Haitao S. 16S rRNA-Base Analysis of Bacteroidetes and Firmicutes Diversity in the Microbial Flora of the Red-eared Slider (Trachemys scripta elegans) Intestinal Tract. Genomics & Applied Biology. 2013; 32: 700–706.

[19] Lu P, Wang F, Wu J, Wang C, Yan J, Li ZL, *et al*. Elevated Serum miR-7, miR-9, miR-122, and miR-141 Are Noninvasive Biomarkers of Acute Pancreatitis. Disease Markers. 2017; 2017: 7293459.

[20] Liu P, Xia L, Zhang WL, Ke HJ, Su T, Deng LB, *et al*. Identification of serum microRNAs as diagnostic and prognostic biomarkers for acute pancreatitis. Pancreatology: Official Journal of the International Association of Pancreatology (IAP). 2014; 14: 159–166.

[21] Xiang H, Tao X, Xia S, Qu J, Song H, Liu J, *et al*. Targeting MicroRNA Function in Acute Pancreatitis. Frontiers in Physiology. 2017; 8: 726.

[22] Hu MX, Zhang HW, Fu Q, Qin T, Liu CJ, Wang YZ, *et al*. Functional role of MicroRNA-19b in acinar cell necrosis in acute necrotizing pancreatitis. Journal of Huazhong University of Science and Technology. Medical Sciences. 2016; 36: 221–225.

[23] Zhu H, Huang L, Zhu S, Li X, Li Z, Yu C, *et al*. Regulation of autophagy by systemic admission of microRNA-141 to target HMGB1 in l-arginine-induced acute pancreatitis *in vivo*. Pancreatology: Official Journal of the International Association of Pancreatology (IAP). 2016; 16: 337–346.

[24] Huang S, Ge X, Yu J, Han Z, Yin Z, Li Y, *et al*. Increased miR-124-3p in microglial exosomes following traumatic brain injury inhibits neuronal inflammation and contributes to neurite outgrowth *via* their transfer into neurons. FASEB Journal: Official Publication of the Federation of American Societies for Experimental Biology. 2018; 32: 512–528.

[25] Sun Y, Li Q, Gui H, Xu DP, Yang YL, Su DF, *et al*. MicroRNA-124 mediates the cholinergic anti-inflammatory action through inhibiting the production of pro-inflammatory cytokines. Cell Research. 2013; 23: 1270–1283.

[26] Nakamachi Y, Ohnuma K, Uto K, Noguchi Y, Saegusa J, Kawano S. MicroRNA-124 inhibits the progression of adjuvant-induced arthritis in rats. Annals of the Rheumatic Diseases. 2016; 75: 601–608.

[27] Fang Y, Hong X. miR-124-3p Inhibits Microglial Secondary Inflammation After Basal Ganglia Hemorrhage by Targeting TRAF6 and Repressing the Activation of NLRP3 Inflammasome. Frontiers in Neurology. 2021; 12: 653321.

[28] Xu Y, Liu N, Wei Y, Zhou D, Lin R, Wang X, *et al*. Anticancer effects of miR-124 delivered by BM-MSC derived exosomes on cell proliferation, epithelial mesenchymal transition, and chemotherapy sensitivity of pancreatic cancer cells. Aging. 2020; 12: 19660–19676.

[29] Wu DH, Liang H, Lu SN, Wang H, Su ZL, Zhang L, *et al*. miR-124 Suppresses Pancreatic Ductal Adenocarcinoma Growth by Regulating Monocarboxylate Transporter 1-Mediated Cancer Lactate Metabolism. Cellular Physiology and Biochemistry: International Journal of Experimental Cellular Physiology, Biochemistry, and Pharmacology. 2018; 50: 924–935.

[30] Wen C, Sun H, Pan K, Sun H, Zhang Z, Cao G, *et al*. Molecular Mechanism Exploration of Pancreatitis Based on miRNA Expression Profile. Clinical Laboratory. 2019; 65.

[31] Carrasco C, Holguín-Arévalo MS, Martín-Partido G, Rodríguez AB, Pariente JA. Chemopreventive effects of resveratrol in a rat model of cerulein-induced acute pancreatitis. Molecular and Cellular Biochemistry. 2014; 387: 217–225.

[32] Kvit KB, Kharchenko NV, Kharchenko VV, Chornenka OI, Chornovus RI, Dorofeeva US, *et al*. The role of small intestinal bacterial overgrowth in the pathogenesis of hyperlipidemia. Wiadomosci Lekarskie (Warsaw, Poland: 1960). 2019; 72: 645–649.

[33] Ren Z, Li Y, Liu J, Li H, Li A, Hong L, *et al*. Coreopsis Tinctoria Modulates Lipid Metabolism by Decreasing Low-Density Lipoprotein and Improving Gut Microbiota. Cellular Physiology and Biochemistry: International Journal of Experimental Cellular Physiology, Biochemistry, and Pharmacology. 2018; 48: 1060–1074.

[34] Fåk F, Bäckhed F. Lactobacillus reuteri prevents diet-induced obesity, but not atherosclerosis, in a strain dependent fashion in Apoe-/- mice. PloS One. 2012; 7: e46837.

[35] Mouries J, Brescia P, Silvestri A, Spadoni I, Sorribas M, Wiest R, *et al*. Microbiota-driven gut vascular barrier disruption is a prerequisite for non-alcoholic steatohepatitis development. Journal of Hepatology. 2019; 71: 1216–1228.

[36] Jayarathne S, Stull AJ, Park OH, Kim JH, Thompson L, Moustaid-Moussa N. Protective Effects of Anthocyanins in Obesity-Associated Inflammation and Changes in Gut Microbiome. Molecular Nutrition & Food Research. 2019; 63: e1900149.

[37] Ruan S, Xu L, Sheng Y, Wang J, Zhou X, Zhang C, *et al*. Th1 promotes M1 polarization of intestinal macrophages to regulate colitis-related mucosal barrier damage. Aging. 2023; 15: 6721–6735.

[38] Zheng L, Xue J, Jaffee EM, Habtezion A. Role of immune cells and immune-based therapies in pancreatitis and pancreatic ductal adenocarcinoma. Gastroenterology. 2013; 144: 1230–1240.

[39] Veremeyko T, Siddiqui S, Sotnikov I, Yung A, Ponomarev ED. IL-4/IL-13-dependent and independent expression of miR-124 and its contribution to M2 phenotype of monocytic cells in normal conditions and during allergic inflammation. PloS One. 2013; 8: e81774.

[40] Yao X, Dong G, Zhu Y, Yan F, Zhang H, Ma Q, *et al*. Leukadherin-1-Mediated Activation of CD11b Inhibits LPS-Induced Pro-inflammatory Response in Macrophages and Protects Mice Against Endotoxic Shock by Blocking LPS-TLR4 Interaction. Frontiers in Immunology. 2019; 10: 215.